Chemistry & Biology
Article

Improved Antifungal Polyene Macrolides via Engineering of the Nystatin Biosynthetic Genes in *Streptomyces noursei*

Trygve Brautaset,[1,5] Håvard Sletta,[1,5] Aina Nedal,[2] Sven Even F. Borgos,[1,2] Kristin F. Degnes,[1] Ingrid Bakke,[3] Olga Volokhan,[3] Olga N. Sekurova,[3] Ivan D. Treshalin,[4] Elena P. Mirchink,[4] Alexander Dikiy,[2] Trond E. Ellingsen,[1] and Sergey B. Zotchev[2,3,*]

[1]Department of Biotechnology, SINTEF Materials and Chemistry, N-7034 Trondheim, Norway
[2]Department of Biotechnology, Norwegian University of Science and Technology, N-7491 Trondheim, Norway
[3]Biosergen AS, N-7465 Trondheim, Norway
[4]Gause Institute of New Antibiotics, 119021 Moscow, Russia
[5]These two authors contributed equally to this work.
*Correspondence: sergey.zotchev@nt.ntnu.no
DOI 10.1016/j.chembiol.2008.08.009

SUMMARY

Seven polyene macrolides with alterations in the polyol region and exocyclic carboxy group were obtained via genetic engineering of the nystatin biosynthesis genes in *Streptomyces noursei*. In vitro analyses of the compounds for antifungal and hemolytic activities indicated that combinations of several mutations caused additive improvements in their activity-toxicity properties. The two best analogs selected on the basis of in vitro data were tested for acute toxicity and antifungal activity in a mouse model. Both analogs were shown to be effective against disseminated candidosis, while being considerably less toxic than amphotericin B. To our knowledge, this is the first report on polyene macrolides with improved in vivo pharmacological properties obtained by genetic engineering. These results indicate that the engineered nystatin analogs can be further developed into antifungal drugs for human use.

INTRODUCTION

Systemic fungal infections represent a serious problem in medical care, as they usually affect patients whose immune systems have been compromised as a result of HIV infection, anticancer therapy, or immunosuppressive therapy after organ transplantation (Sims et al., 2005; Maschmeyer et al., 2007; Silveira and Husain, 2007). The number of antifungal agents that can be used to treat such infections is currently limited to azoles (e.g., voriconazole), echinocandins (e.g., caspofungin), and polyene macrolides (e.g., amphotericin B). All the above-mentioned antifungals have their own therapeutic limitations because of drug-drug interactions, development of resistance, narrow spectrum of activity, and toxicity (Scott and Simpson, 2007; Perlin, 2007; Spanakis et al., 2006; Zotchev, 2003). The polyene macrolide amphotericin B (AmB) has been used for treatment of systemic fungal infections for several decades, showing excellent efficacy against a number of fungal pathogens. At the same time, severe side effects, such as nephrotoxicity, and suboptimal pharmacokinetics, undermine therapeutic value of this antibiotic. A number of AmB analogs, both semisynthetic and genetically engineered, have been generated over the last 20 years in an attempt to reduce its toxicity and improve solubility (Falk et al., 1999; Paquet and Carreira, 2006; Seco et al., 2005; Carmody et al., 2005). Despite that, no new AmB-based antifungal has appeared on the market, except for the lipid and liposomal formulations. However, studies of the AmB analogs have generated important data on the structure-activity relationship of polyene macrolides that may also be at least partially applicable to other scaffolds belonging to the same type of compounds. According to these studies, the exocyclic carboxyl and the amino group of mycosamine seem to be particularly important for selective toxicity and activity (Mazerski et al., 1995; Borowski, 2000). Moreover, Power et al. (2008) have recently generated a mutant of *Streptomyces nodosus* with inactivated ketoreductase (KR) domain in module 16 of the AmB polyketide synthase (PKS) that was shown to produce 7-deoxy-7-oxy AmB. The latter compound has been shown to retain antifungal activity, while having reduced hemolytic activity, compared with that of AmB. To our knowledge, none of these AmB analogs has been tested in vivo.

Polyene macrolides are mostly produced by *Streptomyces* bacteria and exert their fungicidal action via interaction with membrane sterols, resulting in the formation of highly organized hydrophilic channels, through which small molecules and ions can leak out (Ōmura and Tanaka, 1984; Teerlink et al., 1980; Baginski et al., 2006). These antibiotics appear to have a higher affinity toward membranes containing ergosterol (e.g., in fungi and some parasites), compared with cholesterol-containing membranes (mammalian cells) (Gagos et al., 2005). Still, polyene macrolides bind to the cholesterol-containing membranes to some extent, thus causing lysis of particularly vulnerable cells (e.g., in kidneys) and subsequent organ damage.

The polyene macrolide antibiotic nystatin produced by *Streptomyces noursei* ATCC 11455 is an important antifungal agent used in human therapy for treatment of superficial mycoses. Its use for treatment of systemic mycoses is precluded by toxicity,

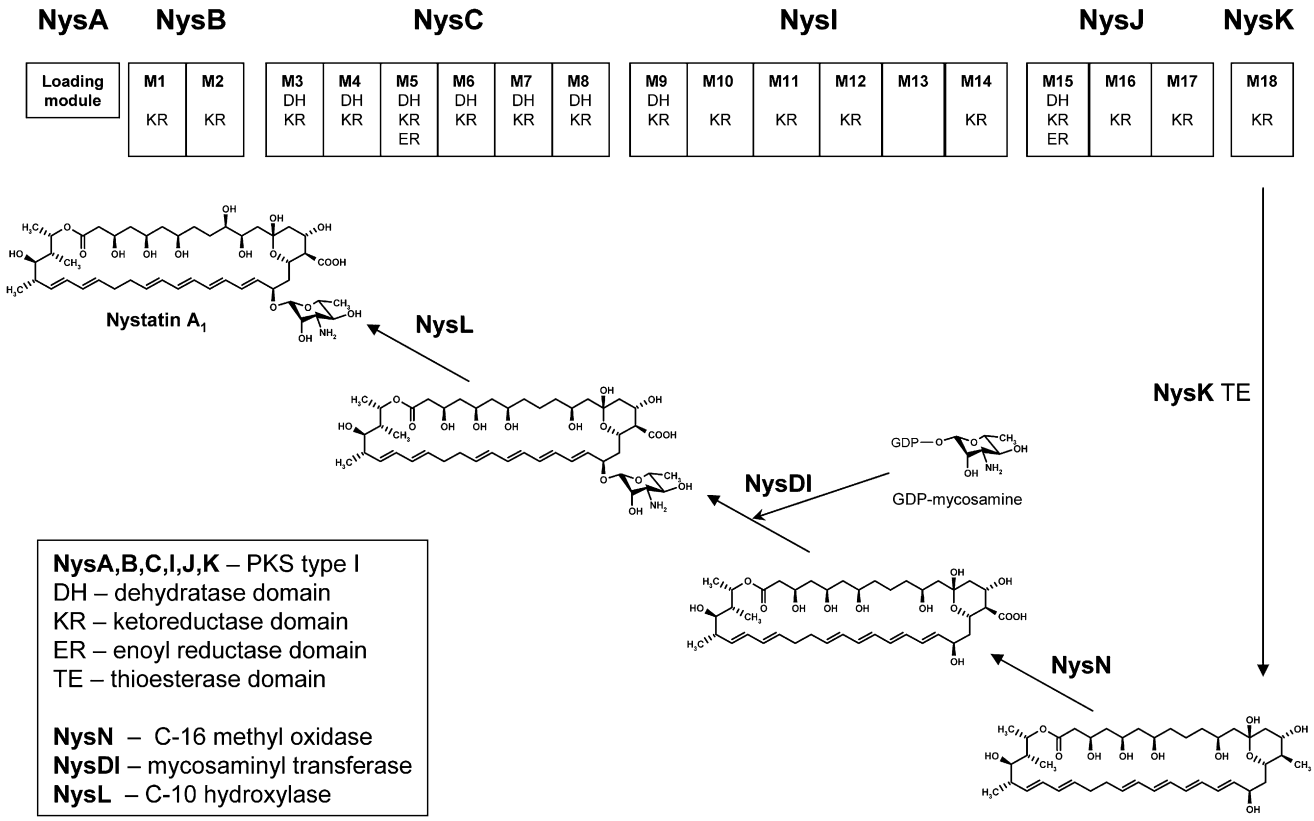

Figure 1. Proposed Nystatin Biosynthesis in *Streptomyces noursei*
Only reductive domains in the nystatin PKS modules are shown.

solubility problems, and lower antifungal activity, compared with that of AmB (Hamilton-Miller, 1973). The nystatin biosynthetic pathway has been established after cloning of the entire biosynthetic gene cluster (Brautaset et al., 2000). It comprises assembly of the 38-member macrolactone ring, followed by oxidation of a C-16 methyl group, attachment of deoxysugar mycosamine at C-19, and hydroxylation at C-10 (Fjærvik and Zotchev, 2005) (Figure 1).

Using genetic engineering, we have recently obtained a heptaene nystatin analog S44HP with antifungal activity considerably higher than that of nystatin and equal to that of AmB (Bruheim et al., 2004). S44HP is structurally similar to AmB but has significantly different properties. For example, S44HP was found to be ~10 times more soluble than AmB and, despite having a lower maximal tolerated dose (MTD) value compared with the latter, seems to have a wider therapeutic window (MTD-LD_{50} dose interval) (Treshchalin et al., 2005). We hypothesized that further derivatization of S44HP might yield new polyene macrolides with improved pharmacological properties, which can be useful for development of safer antifungals. In the present work, we report the generation of new nystatin and S44HP analogs by means of manipulation of the nystatin biosynthetic genes and their biological characterization. Two of these analogs tested in vivo displayed high efficacy and considerably lower acute toxicity, compared with AmB, suggesting that they can become lead compounds for development of new antifungal drugs for human use.

RESULTS AND DISCUSSION

Specific Change in the C-9–C-10 Polyol Region of Nystatin Leads to a Significant Reduction of Hemolytic Activity

The polyol region on the polyene macrolide molecule has recently become a potentially interesting target for modification through biosynthetic engineering. Caffrey and co-workers have demonstrated that replacement of the C-7 hydroxyl group on the AmB molecule with a keto group leads to over 10-fold reduction of in vitro hemolytic activity and ~4-fold reduction of antifungal activity (Power et al., 2008). On the nystatin A_1 molecule, the C-1–C-15 polyol region is interrupted by a saturated C-9–C-10 bond formed as a result of the activity of KR, dehydratase (DH), and enoyl reductase (ER) domains in the module 15 of the nystatin PKS NysJ (Figure 1). To gain a better insight into structure-activity relationship of nystatin, we inactivated DH15 domain of NysJ by site-specific mutagenesis of the active site His followed by gene replacement in *S. noursei* NDA59, yielding mutant NJDH15 (see Table S1 available online). The host strain NDA59 has a *nysA* deletion, and nystatin production can be restored to almost 100% by complementation with *nysA* gene (Brautaset et al., 2003).

Mutant NJDH15 was complemented with the *nysA* gene, cultivated in the fermentor, and DMSO extracts were assayed for polyene production by liquid chromatography (LC)-diode array detector (DAD)-time of flight (TOF). The analysis unraveled the

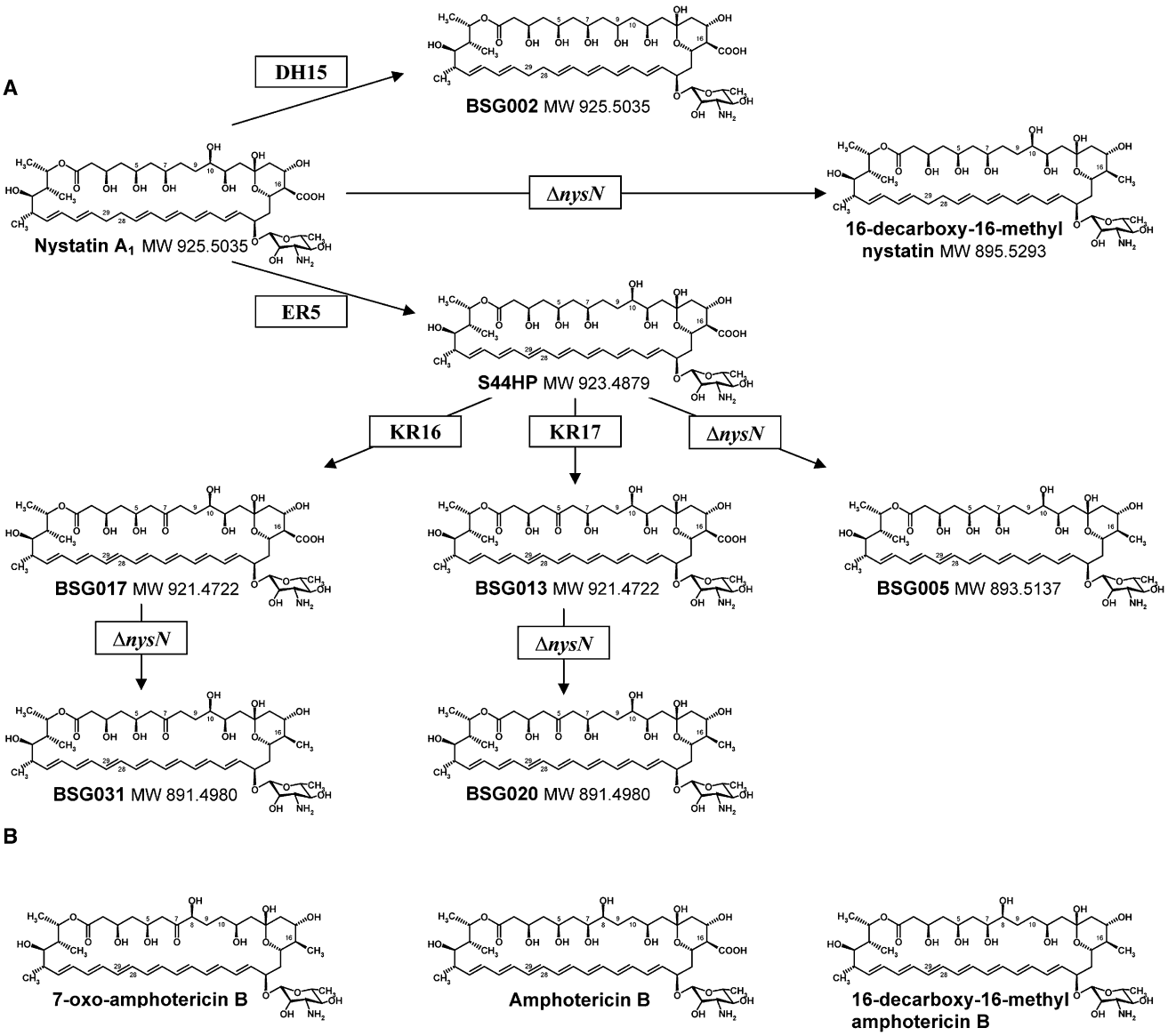

Figure 2. Genetically Engineered Polyene Macrolides

(A) Molecular structures of nystatin and its analogs generated by biosynthetic engineering.

(B) Molecular structures of amphotericin B analogs produced via manipulation of biosynthetic genes (Carmody et al., 2005; Power et al., 2008).

production of an analog with a mass (m/z) corresponding to the stoichiometric formula of nystatin (less than 2 ppm difference from the theoretical mass) in both ESI+ (positive ionization) and ESI− (negative ionization) modes (Figure S1). The volumetric production yield of this analog, denoted BSG002 (0.88 ± 0.04 g/l) was about 30% of the nystatin production level obtained in the wild-type strain under the same conditions (Table S2).

Since the expected change shall affect the C-9–C-10 region, we hypothesized that the NysL hydroxylase (Volokhan et al., 2006) might not recognize the altered C-9–C-11 region on the new molecule, thus failing to perform C-10 hydroxylation. Thus, a new analog with a molecular weight identical to that of nystatin can be explained if this compound has acquired a C-9 hydroxyl, but lacks C-10 hydroxyl group. To verify this hypothesis, the major compound produced by the NJDH15 mutant was purified using preparative high-pressure liquid chromatography (HPLC), and the concomitant nuclear magnetic resonance (NMR) analysis (see Supplemental Text and Figure S2) clearly supported our hypothesis that BSG002 indeed represents 9-hydroxy-10-deoxy nystatin (Figure 2).

Purified BSG002 (purity >95% and concentration of active principle adjusted according to the purity) was then subjected to the in vitro tests for antifungal and hemolytic activities (see Experimental Procedures). BSG002 was found to be at least 2-fold less hemolytic, compared with nystatin. However, its antifungal activity was simultaneously reduced ~4-fold (Table 1). According to the model of the channel formed by polyene macrolides, the hydroxyl groups in the polyol region create a hydrophilic

Table 1. In Vitro Determined Antifungal and Hemolytic Activities of the Genetically Engineered Nystatin Analogs

Compound	MIC_{50} (μg/ml) [a]	MIC_{90} (μg/ml) [a]	HC_{50} (μg/ml) [b]
Nystatin	1.2 ± 0.2	2.0 ± 0.3	85
BSG002	4.8 ± 0.4	10.5 ± 3.5	180
16-DecNys	1.3 ± 0.4	1.8 ± 0.5	175
AmB	0.12 ± 0.03	0.19 ± 0.03	2.6
S44HP	0.12 ± 0.03	0.20 ± 0.03	2.5
BSG005	0.07 ± 0.02	0.12 ± 0.03	4.0
BSG013	0.25 ± 0.07	0.43 ± 0.07	3.0
BSG017	0.47 ± 0.15	0.92 ± 0.03	3.3
BSG020	0.15 ± 0.03	0.19 ± 0.03	9.0
BSG031	0.18 ± 0.06	0.37 ± 0.07	3.8

The ± values represent maximum deviation from the mean.
[a] Tested as described in Nedal et al., (2007) using *Candida albicans* ATCC 10231 as a test organism.
[b] Tested by using horse blood erythrocytes and antibiotic concentrations ranging between 0 and 200 μg/ml.

environment allowing for leakage of ions from the affected cells. One could expect that the addition of a hydroxyl group at C-9 might increase the conductance of the channel, and hence increase antifungal activity, while removal of C-10 hydroxyl should have no effect, as suggested by the data on 10-deoxy nystatin (Volokhan et al., 2006).

Replacement of the C-16 Carboxyl on the Nystatin Molecule with a Methyl Group Reduces Hemolytic Activity Without Affecting the Antifungal Activity

Replacement of a C-16 carboxyl with a methyl group on the AmB molecule by means of inactivation of the methyl oxidase AmphN yielded a less hemolytic analog with retained antifungal activity (Carmody et al., 2005). The *S. noursei* nystatin gene cluster contains a *nysN* gene encoding a putative P450 monooxygenase earlier implicated in oxidation of the C-16 methyl to afford a carboxyl group on the mature antibiotic molecule (Brautaset et al., 2000). Accordingly, *S. noursei* mutant CL346AS, carrying a mutation in the *nysN* gene replacing the conserved Cys residue (Cys346) of NysN presumed to be responsible for heme binding with Ala, was constructed (Table S1). This mutation was predicted to abolish activity of NysN on the basis of the data reported for another P450 monooxygenase (Vatsis et al., 2002). Mutant strain CL346AS was cultivated in the fermentor and analyzed for production of polyene macrolides, as described above. The expected mass corresponding to the stoichiometric formula of 16-decarboxy-16-methyl nystatin ($C_{47}H_{77}NO_{15}$) was identified (<3 ppm difference from the theoretical mass) in both ESI+ and ESI− modes in the culture extract (Figure S3). The production level of 16-decarboxy-16-methyl nystatin (16-DecNys) was very low (0.06 ± 0.01 g/l) and represented less than 2%, compared with the nystatin production in the wild-type strain (Table S2). Similarly low production yield of 16-decarboxy-16-methyl AmB analog has been observed in *S. nodosus* upon inactivation of the *amphN* gene (Carmody et al., 2005). Since we did not observe any abnormal growth for the CL346AS mutant, it seems unlikely that 16-DecNys is toxic to the producing organism. Potentially, accumulation of the latter analog may cause feedback inhibition of the nystatin biosynthetic pathway by an unknown mechanism (see below).

In vitro hemolytic assay of the purified 16-DecNys (purity 75% and concentration of active principle adjusted according to the purity) revealed about 2-fold increased HC_{50} value for this compound, compared with the parental antibiotic nystatin (Table 1). At the same time, its antifungal activity remained unchanged, as judged from the MIC_{50}/MIC_{90} values for *Candida albicans*, which were 1.2 ± 0.2/2.0 ± 0.3 μg/ml and 1.3 ± 0.4/1.8 ± 0.5 μg/ml for nystatin and 16-DecNys, respectively (Table 1). Combined, these data imply that replacement of the C-16 carboxyl with a methyl group reduces the toxicity of nystatin, while having no effect on its antifungal activity. These data are in good agreement with the analogous result previously documented for 16-decarboxy-16-methyl AmB (Carmody et al., 2005). Because of the low yield, we were unable to produce 16-DecNys in quantity and purity sufficient for NMR analysis of the structure and in vivo animal experiments.

C-16 Modification of the Heptaene Nystatin Analog S44HP Yields Less Hemolytic and More Active Polyene Macrolide

Encouraged by the in vitro data obtained for 16-DecNys (see above), we introduced identical C-16 modification on the molecule of the heptaene nystatin analog S44HP, which was shown to have 6-fold higher in vitro antifungal activity than nystatin (Bruheim et al., 2004). The CL346AS mutation in the *nysN* gene was introduced into the S44HP-producing mutant *S. noursei* GG5073SP (Borgos et al., 2006a), generating mutant BSM1 (Table S1). BSM1 was cultivated in the fermentor and assayed for polyene macrolides by LC-DAD-TOF. The expected mass corresponding to the stoichiometric formula of 16-decarboxy-16-methyl-28,29-didehydro nystatin ($C_{47}H_{75}NO_{15}$), was identified in the culture extract (<1.5 ppm difference from the theoretical mass) in the ESI− mode (Figure S4), and this compound was designated BSG005 (Figure 2). Interestingly, the BSG005 production level by BSM1 in the fermentor (0.53 ± 0.01 g/l) was about 40%, compared with the S44HP production level by parental strain GG5073SP (Table S2). This was ~20 times higher than the relative production level of 16-DecNys by the analogous *nysN* mutant CL346AS constructed on the wild-type background (see above), and the biological reason for this discrepancy is unknown. It is possible that the C28-29 double bond in BSG005 somehow negatively affects its ability to inhibit the nystatin biosynthetic pathway, whereas 16-DecNys, which has a saturated C28-C29 bond, has much higher potential for inhibiting the pathway. Chemical structure of the expected BSG005 analog, 16-decarboxy-16-methyl-28,29-didehydro nystatin, was confirmed by NMR experiments on purified compound (Figures S5 and S6).

In vitro assay for the purified BSG005 (purity >95%) revealed its ~2-fold and 20-fold increased antifungal activity, compared with S44HP and nystatin, respectively (Table 1; Figure S7). At the same time, its hemolytic activity was reduced ~1.5-fold, compared with S44HP (Table 1). Together, these data imply that replacement of the C16-carboxyl group on S44HP with a methyl has a positive effect on the pharmacological properties of this compound under the conditions tested. These results are in agreement with the similar data reported for noncarboxylated analogs of both AmB and rimocidin (Seco et al., 2005; Carmody

et al., 2005; Palacios et al., 2007), although the MIC values for the latter two compounds have not been reported.

C-5 and C-7 Keto Modifications in the S44HP Polyol Region Yield Analogs with Reduced Antifungal and Hemolytic Activities

According to the current model, the polyol regions of antibiotic molecules with multiple hydroxyl groups outline the inner part of the channel piercing the target cell membrane (Baginski et al., 2002). The hydrophilic properties of the channel are most likely affected by the number and position of the hydroxyls, and thus variation of these properties might theoretically affect the channel's ion selectivity and conductivity. Power et al. (2008) have reported biosynthetic engineering of the 7-oxo-AmB analog with reduced hemolytic activity. We decided to generate S44HP analogs, where either C-5 or C-7 hydroxyls in the polyol region were replaced with keto groups, and to compare their biological properties. The KR17 domain of the nystatin PKS NysJ protein is responsible for catalyzing the reduction the C-5 keto group to afford the C-5 hydroxyl during the biosynthesis of the nystatin macrolactone ring (Brautaset et al., 2000) (Figure 1). To generate an S44HP analog with retained C5-keto group, we introduced the double mutation TA5145FE affecting the proposed KR17 active site Tyr residue in the nystatin PKS NysJ. The KR16 domain of the NysJ PKS is responsible for catalyzing the reduction the C-7 keto group to afford the C-7 hydroxyl on the nystatin molecule. To generate an S44HP analog with retained C7-keto group, we introduced the double mutation YA3404FE affecting the KR16 active site Tyr3404 residue in NysJ. The KR17 and KR16 mutations were individually introduced to the *S. noursei* mutant GG5073SP, generating mutants BSM2 and BSM4, respectively (Table S1).

The two latter strains were cultivated in the fermentor and assayed for polyene macrolides by LC-DAD-TOF. Accurate masses, which correlated well with the expected 5-oxo-5-deoxy-28,29-didehydro nystatin and 7-oxo-7-deoxy-28,29-didehydro nystatin (both with stoichiometric formula $C_{47}H_{71}NO_{17}$) were found in ESI− and ESI−/ESI+ modes, respectively, (<5 ppm difference from the theoretical mass, Figures S8 and S9). The compounds produced by the BSM2 and BSM4 mutants were designated BSG013 and BSG017, respectively (Figure 2). The volumetric production yields of BSG013 (0.73 ± 0.01 g/l) and BSG017 (0.63 ± 0.07 g/l) correspond to about 56% and 49%, respectively, of the S44HP production yield obtained for the parental strain GG5073SP (Table S2). Chemical structure of BSG013 was also confirmed by NMR experiments (Figure S5). Structurally, BSG013 and BSG017 seem to be identical to the previously reported polyene macrolides mycoheptin (Borowski et al., 1978) and candidin (Volpon and Lancelin, 2002), respectively.

Next, purified BSG013 and BSG017 (purity >95%) were tested in vitro for hemolytic and antifungal activities, as described above. Compared to S44HP, BSG013 showed ~2-fold reduced antifungal activity with concomitantly 1.2-fold increased HC_{50} value (Table 1; Figure S7). BSG017 showed a 4-fold reduced antifungal activity and 1.3-fold increased HC_{50} value compared to S44HP (Table 1; Figure S7). These data indicated that substitutions of C-5 or C-7 hydroxyls with keto groups reduce both antifungal and hemolytic activities of the S44HP analogs. These data were consistent with those reported for 7-oxo AmB analog, where reduction of both antifungal and hemolytic activities have been observed (Power et al., 2008). However, reduction of hemolytic activity upon replacement of C-5 and C-7 hydroxyls with keto groups on S44HP was not as dramatic as in the case of 7-oxo AmB.

Combination of C-16 with C-5 or C-7 Keto Modifications on S44HP Results in Analogs with Further Reduced Hemolytic Activity and High Antifungal Activity

Considering that BSG005, BSG013, and BSG017 were all less hemolytic than S44HP in vitro, we decided to combine the corresponding modifications on these molecules in an attempt to obtain an analog with further reduced toxicity. The CL346AS *nysN* mutation that was used to construct mutant BSM1 was introduced into the BSG013- and BSG017-producing mutants BSM2 and BSM4, yielding recombinant strains BSM3 and BSM5, respectively (Table S1). The two latter strains were cultivated in the fermentor, and production of polyene macrolides was assessed by LC-DAD-TOF. Accurate masses which correlated well with the 5-oxo-5-deoxy-16-decarboxy-16-methyl-28,29-didehydro nystatin and 7-oxo-7-deoxy-16-decarboxy-16-methyl-28,29-didehydro nystatin (both with stoichiometric formula $C_{47}H_{73}NO_{15}$), were found in ESI− and ESI+ modes (all with <3 ppm difference from the theoretical masses, Figures S10 and S11). The analogs identified were designated BSG020 and BSG031, respectively (Figure 2). In addition, tandem mass spectrometer (MS)-MS data were used to confirm the chemical structure of BSG020 (Figure S12). The volumetric production yields of BSG020 (0.26 ± 0.02 g/l) and BSG031 (0.37 ± 0.04 g/l) corresponded to ~20% and 29%, respectively, of that of S44HP produced by the parental strain GG5073SP (Table S2). These data demonstrate that several alterations can simultaneously be introduced into the nystatin biosynthetic pathway without dramatically affecting production yields of new analogs.

The purified compounds BSG020 and BSG031 (93% and 80% pure, respectively) were subjected to in vitro activity and toxicity assays as described above. The data from these experiments showed that BSG020 and BSG031 had ~3.5- and 1.5-fold increased HC_{50} values, compared with S44HP, respectively, and that their antifungal activities were improved compared to those of their parental oxo-analogs. (Table 1 and Figure S7). Together, these data indicate that the combination of the oxo substitutions in the polyol region and C-16 methyl group can potentially be beneficial for improvement of therapeutic index of S44HP. It should be noted that AmB analogs with combined C-15-oxo and C-16-methyl modifications have been obtained by Power et al. (2008). Unfortunately, yields of these analogs had apparently been too low for purification of substantial amounts of materials, although crude samples clearly exhibited antifungal activity. We have failed to generate a mutant producing C-15-oxo analog of S44HP in detectable amounts, although two alternative mutations for KR12 inactivation in the nystatin PKS NysI were attempted (data not shown).

BSG005 and BSG020 Have Considerably Reduced Toxicity, and BSG005 also Displays Improved Antifungal Activity, Compared with AmB In Vivo

On the basis of all the accumulated in vitro data (see above), one nystatin analog (BSG002) and two S44HP analogs (BSG005 and

Table 2. In Vivo Acute Toxicity and Antifungal Activity of Engineered Nystatin Analogs Tested in a Mouse Model of Disseminated Candidosis

Compound	MTD mg/kg	LD_{50} mg/kg	*Candida* kidney load, CFU/g (% MTD)[a,b]
Control	NA	NA	6.5×10^4
Nystatin	7.1	8.5	3.4×10^3 (56%)
BSG002[c]	53.7	61.7	6.3×10^4
S44HP	0.6	2.1	4.2×10^3 (94%)
BSG005	7.8	15.4	2.9×10^3 (10%)
BSG020	7.9	10.5	6.5×10^3 (10%)
AmB	2.0	2.8	4.0×10^3 (40%)

[a] After 4 days of single dose administration of 0.8 mg/kg, except for nystatin (4 mg/kg), BSG002 (32 mg/kg) and S44HP (0.6 mg/kg).
[b] Average data for 3 animals.
[c] No activity demonstrated for doses up to 32 mg/kg.

BSG020) were chosen for in vivo studies on acute toxicity and antifungal activity against disseminated candidosis in a mouse model. First, BSG002 was investigated and compared to its parental compound nystatin. Preparations containing different antibiotic concentrations were administered intravenously, and median lethal and maximum tolerated doses (LD_{50} and MTD values, respectively) were calculated from the experimental data. BSG002 was shown to have considerably lower acute toxicity than nystatin in these experiments; the MTD/LD_{50} values for BSG002 and nystatin were 53.7/61.7 mg/kg and 7.1/8.5 mg/kg, respectively (Table 2). These data were in good agreement with the corresponding in vitro data (Table 1). BSG002 and nystatin were then used in a mouse candidosis model in order to assess their antifungal activity in vivo (see Experimental Procedures). The fungal load in the kidneys of *C. albicans* infected animals treated with antibiotics was determined and compared with that of the untreated animals. In this experiment, nystatin demonstrated in vivo antifungal activity (reduction of *Candida* colony-forming units [CFU] in kidneys by a factor of >10) at doses equal or higher than 4 mg/kg, whereas no activity was shown for BSG002 at doses up to 32 mg/kg (Table 2). The fact that BSG002 lacks activity in a mouse model of candidosis, while having reduced but still significant activity in vitro, suggests that such factors as stability in vivo and pharmacokinetics might play a decisive role for therapeutic usefulness of polyene macrolides.

Next, BSG005 and BSG020 were tested in similar experiments, and the data obtained for both analogs clearly demonstrated higher MTD and LD_{50} values, compared with those for both S44HP and AmB, suggesting that they have considerably lower toxicity in vivo (Table 2). Compared with S44HP, the MTD value was increased ~13-fold for both BSG005 and BSG020, indicating significant reduction of toxicity. These data were in some agreement with the in vitro data on hemolytic activities of these compounds, whereas the effects in vivo were much more profound (Table 1). When assessed for efficacy in a mouse candidosis model, the effective doses for AmB, S44HP, BSG005, and BSG020 (Table 2) were considerably lower than that for nystatin and correlated well with the in vitro data for antifungal activity as presented in Table 1. BSG005 displayed in vivo antifungal activity slightly higher than those of both AmB and S44HP, whereas the antifungal activity of BSG020 was somewhat reduced compared to these control compounds. Again, these data were in agreement with the in vitro antifungal activity tests showing that BSG020 displays a lower antifungal activity than does BSG005 (Table 1). Most importantly, these in vivo antifungal activities were observed at doses corresponding to only ~10% of MTD for both BSG005 and BSG020. At the same time, 40% and 94% MTD doses for AmB and S44HP, respectively, had to be used to achieve the same efficacy in reducing fungal kidney load. The latter data confirm that both BSG005 and BSG020 have favorable activity/toxicity properties, compared with AmB, under these conditions and suggest that they may become promising lead compounds for further development as antifungal agents.

Structure-Activity-Toxicity Relationship of Engineered Nystatin Analogs

The impact of modifications introduced into three different regions of the nystatin molecule on its antifungal activity and toxicity has been investigated both in vitro and in vivo in this study. In particular, the polyene region (C-28–C-29), the exocyclic carboxyl group (C-16), and the polyol region (C-5, C-7, C-9, and C-10) were targeted for modifications. The data obtained for S44HP supports our previous observation (Bruheim et al., 2004) that modification of the polyene region resulting in the appearance of seven instead of four conjugated double bonds increases both antifungal activity and toxicity. This result is consistent with significantly higher antifungal activity and toxicity reported for the heptaene polyene macrolide AmB, compared with that of nystatin. The data obtained for C-16 methyl substituted S44HP analog demonstrated that this modification leads to increased antifungal activity and reduced toxicity, whereas the analogous modification reported for AmB caused reduced toxicity while leaving antifungal activity presumably unchanged (Carmody et al., 2005). Modifications in the polyol region of nystatin (C-5, C-7, and C9+C10) yielded compounds with both reduced antifungal activity and toxicity, whereas the effect varied among these modifications. Interestingly, the C-7 modification in AmB (Power et al., 2008) had no effect on antifungal activity, while causing reduced toxicity, thus further confirming differences between AmB and S44HP in terms of structure-activity relationship. Taken together, our data suggest that the polyol and polyene region, as well as C-16 exocyclic, are all important for the antifungal activity and toxicity of nystatin and S44HP. Moreover, our data obtained for the analogs combining different modifications indicate that simultaneous introduction of C-16 methyl and C-5 keto group on S44HP may be beneficial for the activity/toxicity profile. Although some of these results could potentially have been expected on the basis of the data available for the genetically engineered AmB analogs (Carmody et al., 2005; Power et al., 2008), certain modifications in the polyol region of nystatin, such as at C-7 and C-9/C-10, had a significant negative effect on antifungal activity, while contributing little to the reduction of toxicity.

SIGNIFICANCE

There is an urgent need for efficient and safe antifungal agents because of the growing number of life-threatening systemic fungal infections. Polyene macrolide antibiotics

are potent fungicidal agents, but their medical usefulness is hampered by considerable toxicity. A series of new analogs of the polyene macrolide antibiotic nystatin was generated by means of biosynthetic engineering. Testing of these analogs in vitro for antifungal and hemolytic activities provided important new data on structure-activity-toxicity relationship and allowed selection of the most active and least toxic analogs. In vivo experiments in a mouse model revealed that two new nystatin analogs, BSG005 and BSG020, are at least as efficient as AmB, the only polyene macrolide currently used for treatment of systemic fungal infections, against disseminated candidosis, while being considerably less toxic. The two analogs might therefore represent promising lead compounds for further development of antifungal drugs for human therapy.

EXPERIMENTAL PROCEDURES

Bacterial Strains, Media, and Growth Conditions

Plasmids, phages, and bacterial strains used in the present study are described in Table S1. *S. noursei* and *Escherichia coli* strains were maintained and genetically manipulated as described elsewhere (Sekurova et al., 1999; Sambrook et al., 1989). Cultivations of *S. noursei* strains for production of analogs were performed in fed-batch fermentation essentially as described elsewhere (Borgos et al., 2006a), except for the use of SAO-50 medium, which contained double amounts of all nutrients, compared to SAO-40 (Borgos et al., 2006a). Analysis of polyene macrolides produced was done as reported elsewhere (Bruheim et al., 2004). The gene replacements were performed through conjugation of the corresponding vectors (see below) into the *S. noursei,* verification of chromosomal integration, and selection for double homologous recombination, as described elsewhere (Sekurova et al., 1999). Gene replacements were performed in *nysA*-deficient mutants NDA59 (Brautaset et al., 2003) and GG5073SP (Borgos et al., 2006a), and the resulting recombinant strains were complemented with the *nysA* gene to restore the polyene macrolide biosynthesis.

DNA Manipulation, Sequencing, and PCR

General DNA manipulations were performed as described elsewhere (Sambrook et al., 1989). DNA fragments from agarose gels were purified using QIAEX II kit (QIAGEN, Germany). Southern blot analyses were performed with the digoxigenin-11-dUTP High Prime labeling kit (Roche Molecular Biochemicals) according to the manufacturer's instruction. Oligonucleotide primers were purchased from MWG Biotech (Germany). The PCRs were performed with the GC Rich PCR System (Roche Molecular Biochemicals) on Eppendorf Mastercycler (Eppendorf, Germany), using conditions described elsewhere (Brautaset et al., 2003). DNA sequencing was performed at MWG Biotech (Germany).

Construction of Gene Replacement Vectors

Inactivation of NysJ DH15

The 3.33 kb *Bcl*I/*Sph*I fragment of recombinant phage N20 (Table S1) was ligated into the *Bam*HI/*Sph*I sites of pGEM-11zf+. From the resulting plasmid, the 3.34 kb *Eco*RI/*Hin*dIII fragment was isolated and ligated into the corresponding sites of plasmid pGEM-3zf+, yielding pDH15-B. The latter plasmid was used as a template for site-directed mutagenesis to introduce the DH15 mutation H966F using the mutagenic oligonucleotides Mut-DH15-1: 5′-CACC CCTGGCTCGCCGACT**TC**GTCGTCGGCGGCATGGTC−3′ (sense) and Mut-DH15-2: 5′-GACCATGCCGCCGACGAC**GA**AGTCGGCGAGCCAGGGGTG−3′ (antisense). Altered nucleotides are indicated in bold, and the introduced mutation eliminated the originally present *Brt*I recognition site (not shown). Mutation was first confirmed by *Brt*I restriction digestion and then verified by DNA sequencing. The plasmid-containing mutation was designated pDH15-mut. The 1.6 kb *Eco*RI/*Sac*I fragment of pDH15-B, the 1.1 kb *Hin*dIII/*Bgl*II fragment of pDH15-B, and the mutated 0.64 kb *Sac*I/*Bgl*II fragment from pDH15-mut were isolated and ligated together with the 3.1 kb *Eco*RI/*Hin*dIII fragment of pSOK201 (Zotchev et al., 2000) (Table S1), yielding DH15 inactivation vector pSH15-123.

Inactivation of nysN

The 4.1 kb *Nco*I/*Xba*I fragment from the recombinant phage N95 (Table S1) was cloned into the corresponding sites of the plasmid pLITMUS28. From the resulting construct, the entire 4.1 kb insert was excised with *Eco*RI/*Hin*dIII and cloned into the corresponding sites of pGEM11-zf+. From the resulting plasmid, pGEM11nysN4.1, the 1.5 kb region including the *nysN* active site was PCR-amplified with primers conA-1F: 5′-TTTTGAATTCTTCAAGCCGATGAGC C-3′ and conA-1R: 5′-TTTTAAGCTTGGTCGAAC AGGTCCGG-3′, introducing *Eco*RI and *Hin*dIII sites (underlined) into the PCR product. These sites were used to clone the PCR fragment into pGEM11-zf+, yielding plasmid pGEM11nysN1.5. The latter plasmid was used as a template for site-directed mutagenesis (QuickChange kit, Stratagene) to introduce *nysN* mutations CL346AS using the oligonucleotides CL346AS-F: 5′-TCGGCTACGGTGTCCAC**GCTAGC**CT GGGCCAGAAC CTGG-3′ and CL346AS-R: 5′-CCAGGTTCTGGCCCAG**GC TAGC**GTGGACACCGTAG CCGA-3′. Altered nucleotides are indicated in bold while the new *Nhe*I restriction site introduced is underlined. Mutation was first confirmed by restriction analysis and then verified by DNA sequencing. The mutated 1.3 kb *Fsp*AI/*Bpu*1102I fragment from the resulting plasmid was cloned back into the corresponding sites of pGM11nysN4.1, yielding pGM11nysN4.1-CL346AS. From the latter construct, the 4.1 kb insert containing mutated *nysN* genes was excised with *Eco*RI/*Hin*dIII and ligated with the 3.1 kb *Eco*RI/*Hin*dIII fragment of pSOK201, yielding plasmid pKOnysN-CL346AS, which was used for *nysN* replacement in *S. noursei*.

Inactivation of NysJ KR17

The 4.0 kb *Pml*I/*Bam*HI fragment from the recombinant phage N98 (Table S1) was excised and ligated into the *Hin*cII/*Bam*HI sites of vector pGEM3-zf+, yielding plasmid pBB4.0. A 1.5 kb DNA fragment, including the KR17 active site region, was PCR amplified from pBB4.0 using primers KR17-F: 5′-TTTT CTGCAGGCCGCGGTGCGCGC-3′ and KR17-R: 5′-TCCGGC ATGGTCCGTG AAACC-3′. The PCR product was digested with *Pst*I (site underlined) and *Sac*I (recognition site in the amplified DNA fragment), and the 1.4 kb fragment was ligated into the corresponding sites of pLITMUS28. The resulting plasmid, pLIT1.4, was used as a template for site-directed mutagenesis with oligonucleotides KR17-mut1: 5′-GCCCCGGCCAGGGCA AC**TT**CG**AA**GCCGGCAACAC GTTCC-3′ and KR17-mut2: 5′-GGAACGTGTTGCCGG C**TT**CGA**A**GTTGCCCT GGCCGGGGC-3′. Altered nucleotides are indicated in bold while new *Bst*BI restriction site introduced is underlined. Correct mutation was verified with *Bst*BI digestion, and the entire insert of the mutated plasmid was verified by DNA sequencing. From the resulting plasmid, pLIT1.4 m, the 1072 bp *Bcl*I/*Acc*III fragment, was excised and used to replace the corresponding fragment in pBB4.0, yielding plasmid pBB4.0 m. The entire 4.0 insert of pBB4.0 m was excised with *Eco*RI and *Hin*dIII and ligated together with the 3.1 kb *Eco*RI/*Hin*dIII fragment of pSOK201, yielding the KR17 inactivation vector pKR17m.

Inactivation of NysJ KR16

The 14 kb *Xba*I insert of the recombinant phage N20 (Table S1) was ligated into plasmid pGEM-3zf, and from the resulting plasmid, pL20X, the 3.7 kb *Bam*HI fragment was excised and ligated into pGEM-3zf+, yielding plasmid pGEMB3.7. A 0.8 kb DNA fragment (encompassing the codon for the KR16 active site residue Y3404) was PCR-amplified from pGEMB3.7 with primers KR16-F1: 5′-ttttctgCAGCCGACCGGCACCGTCC-3′, and KR16-R: 5′-tttt aaGCTTCCTGGAC CGCGCGGG-3′. The PCR product was digested with *Pst*I and *Hin*dIII (recognition sites underlined in the two PCR primers) and ligated into the corresponding sites of pLITMUS28, yielding pLITPH0.8. The latter plasmid served as a template for site-directed mutagenesis to introduce the KR16 double mutation YA3404FE using the mutagenic oligonucleotides mutKR16-1F: 5′-CCCCGGCCAGGCCGGC**TT**CG**AA**GCCG CCAACGCGGTC C-3′ (sense) and mutKR16-1R: 5′-GGACCGCGTTGGCGGC**TT**CG**AA** GCCGG CCTGGCCGGGG-3′ (antisense). Mutated nucleotides are shown in bold, and the new *Bst*BI recognition site introduced is underlined. The correct mutation was identified by *Bst*BI digestion and verified by DNA sequencing. From the plasmid containing desired mutation, the 627 bp *Bpu*102I/*Bpu*10I fragment was excised and used to replace the corresponding fragment in pGEMB3.7, yielding plasmid pGEMB3.7 m. From the latter plasmid, the entire 3.7 kb insert was excised with *Eco*RI/*Hin*dIII and ligated together with the 3.1 kb *Eco*RI/*Hin*dIII fragment of pSOK201, yielding KR16 inactivation vector pKR16m. The latter vector was introduced into the *nysA*-deficient *S. noursei* mutant GG5073SP (Borgos et al., 2006a) by double homologous recombination.

Gene Replacements in *S. noursei* Strains

The constructed gene replacement vectors (see above) were introduced to the *S. noursei* strains by conjugation, and gene replacements were selected after double homologous recombination, as described elsewhere (Sekurova et al., 1999). The correct chromosomal mutations were verified by PCR, DNA sequencing of PCR products, and Southern blot analyses. Polyene macrolide production was restored in the recombinant strains by introducing the *nysA* gene as described elsewhere (Brautaset et al., 2003).

Preparative LC-MS Purification of Genetically Modified Polyenes, MS/MS, and NMR Experiments

The LC-MS-guided purification was performed essentially as described elsewhere (Bruheim et al., 2004; Borgos et al., 2006b), but with methanol instead of acetonitrile as the mobile phase organic constituent (from 70% up to 80% methanol, depending on the polyene to be purified). Purity and concentration of the engineered polyenes was determined by reference to USP standards of nystatin and AmB for tetraenes and heptaenes, respectively, assuming that molar extinction coefficients in the spectral regions of interest were unaltered. Peak UV absorption at 309 nm and 386 nm, arising from the polyene region, was used for tetraenes and heptaenes, respectively. Samples for MS/MS analyses were prepared by dissolving purified compounds in DMSO to a final concentration of 5 mg/ml. The MS/MS analysis was performed using the Agilent 1200 series LC/Qtof system. The eluent was 30% acetonitrile in water at a flow rate of 0.4 ml/min. An Agilent Zorbax Bonus-RP 2.1 × 50 mm column was used. The Qtof mass spectrometer was operated with the electrospray ionization source in positive ionization mode. Drying gas flow was 11 l/min, and nebulizer pressure was 45 psi. Drying gas temperature was 350°C and the fragmentor voltage was 175 V. During MS/MS spectra acquisition, a fixed collision energy of 25 V was used. Samples for NMR spectroscopy were prepared by dissolving freeze-dried compounds purified by preparative HPLC in d_6-DMSO at 1 mM final concentration. To be able to perform direct comparison of NMR assignments reported previously (Bruheim et al., 2004) and obtained in the present study, both sample and further NMR experimental conditions were maintained analogous to those already described. All NMR experiments were recorded at 298 K on a Bruker DRX600 spectrometer equipped with a 5-mm z-gradient TXI (H/C/N) cryogenic probe. Proton and carbon chemical shifts were referenced to TMS signal. To monitor the chemical structure of the investigated compounds, both one-dimensional ^{1}H and two-dimensional COSY and ^{1}H-^{13}C HSQC spectra were recorded. Detailed description and analysis of the results are given in the Supplemental Material.

Determination of In Vitro Antifungal and Hemolytic Activity

Determination of in vitro antifungal activity was done by cultivating *C. albicans* in 96-well plates and monitoring cell growth in the presence of 24 different concentrations of antibiotics, as described elsewhere (Borgos et al., 2006b; Nedal et al., 2007). MIC_{50} and MIC_{90} values, representing minimum inhibitory concentrations causing 50% and 90% inhibition of cell growth, respectively, were calculated from at least 3 parallel experiments. Hemolytic assays for the genetically modified polyene macrolides were performed by monitoring their ability to cause lysis of defibrinated horse blood erythrocytes washed from plasma proteins with PBS buffer, as described elsewhere (Borgos et al., 2006b; Nedal et al., 2007). Antibiotic solutions were prepared in DMSO to achieve final concentrations between 0 and 200 μg/ml, and the mixtures were incubated at 37°C for 1 hr before the optical densities of supernatants at 545 nm were measured. The results presented are mean values from 3 independent measurements. Hemolytic concentrations causing 50% hemolysis, HC_{50} values, were determined from the generated plots (Figure S12).

In Vivo Testing of Acute Toxicity and Antifungal Activity

All animal experiments were performed in accordance with the Guidelines for Drugs Toxicity Testing on Animals approved by the Russian Academy of Medical Sciences (RAMS). Prior to initiation of experiments, the protocols were reviewed and approved by the Ethical Committee of the Gause Institute of New Antibiotics (RAMS). Male mice (weight, 19–22 g) of first generation hybrids BDF1 (C57Bl × DBA2) received from the Central Nursery of RAMS were used in the experiments. The animals were kept on a standard diet consisting of briquette forages with easy access to potable water in the animal nursery of the Gause Institute of New Antibiotics. After the fortnight quarantine, healthy animals were divided into groups with six individuals in each and were entered into the experiments.

Nystatin, AmB, S44HP, BSG002, BSG005, and BSG020 (5 mg) were each mixed with dry sodium deoxycholate (4.1 mg) in a sterile glass vial. Ten milliliters of phosphate buffer (NaH_2PO_4, 1.59 g; Na_2HPO_4, 0.96 g; and H_2O, to 100 ml) was added and immediately subjected to vigorous shaking for 10 min until homogeneous suspensions were formed. The obtained suspensions were placed into the new sterile glass vials, 5% neutral sterile glucose solution was added, and the resulting solutions (up to 0.8 mg/ml) were used for intravenous administration.

Acute Toxicity

Freshly prepared antibiotic solutions were individually injected into the mouse's tail vein at <0.5 ml per minute. Each antibiotic was used in a range of doses resulting in 0% to 100% lethality and a minimum of three intermediate doses. Toxicity-characterizing doses MTD and LD_{50} were calculated with the method of "probit" analysis, according to Litchfield and Wilcoxon (1949), using the statistical analysis program StatPlus (version 3.5.0., 2005).

Antifungal Activity

Mice were infected intravenously with 10^6 CFU of *C. albicans* ATCC 14053 per mouse (0.1 ml). Thirty minutes after infection, antibiotics (six doses, ranging from 1% to 95% MTD, three mice per dose per antibiotic) were administered through the lateral tail vein. Each dose was administered once a day for four days, including the day of infection (0, 1, 2, and 3 days). As a control, a group of untreated infected mice and a placebo group of noninfected animals, which were intravenously administered 0.2 ml of the solvent (phosphate buffer + 5% glucose [1:1]), were used. On the fifth day of the experiment, mice were weighed and sacrificed. The *C. albicans* kidney burden for each mouse was determined by counting CFUs in homogenates from the kidneys. The kidneys were removed aseptically, weighed, and pounded in porcelain mortars with sterile corundum; dilutions of the resulting suspensions were prepared and plated on Sabouraud dextrose agar. The plates were incubated for up to 72 hr at 35°C, colonies of *C. albicans* were counted, and the load was estimated per 1 g of kidney tissue. Statistical analysis was performed with Microsoft Office Excel 2003. Significant distinctions had a $p \leq 0.05$ at comparison by Student T-criterion.

SUPPLEMENTAL DATA

Supplemental Data include Supplemental Experimental Procedures, two tables, and twelve figures and can be found with this article online at http://www.chembiol.com/cgi/content/full/15/11/1198/DC1/.

ACKNOWLEDGMENTS

We thank E. Pereverzeva for help with animal studies. This work was supported by Biosergen AS and the Research Council of Norway.

Received: February 29, 2008
Revised: August 8, 2008
Accepted: August 14, 2008
Published: November 21, 2008

REFERENCES

Baginski, M., Resat, H., and Borowski, E. (2002). Comparative molecular dynamics simulations of amphotericin B-cholesterol/ergosterol membrane channels. Biochim. Biophys. Acta *1567*, 63–78.

Baginski, M., Czub, J., and Sternal, K. (2006). Interaction of amphotericin B and its selected derivatives with membranes: molecular modeling studies. Chem. Rec. *6*, 320–332.

Borgos, S.E.F., Sletta, H., Fjærvik, E., Brautaset, T., Ellingsen, T.E., Gulliksen, O.M., and Zotchev, S.B. (2006a). Effect of glucose limitation and specific mutations in the module 5 enoyl reductase domains in the nystatin and amphotericin polyketide synthases on polyene macrolide biosynthesis. Arch. Microbiol. *185*, 165–171.

Borgos, S.E., Tsan, P., Sletta, H., Ellingsen, T.E., Lancelin, J.M., and Zotchev, S.B. (2006b). Probing the structure-function relationship of polyene

macrolides: engineered biosynthesis of soluble nystatin analogues. J. Med. Chem. *49*, 2431–2439.

Borowski, E. (2000). Novel approaches in the rational design of antifungal agents of low toxicity. Farmaco *55*, 206–208.

Borowski, E., Golik, J., Zieliński, J., Falkowski, L., Kołodziejczyk, P., and Pawlak, J. (1978). The structure of mycoheptin, a polyene macrolide antifungal antibiotic. J. Antibiot. (Tokyo) *31*, 117–123.

Brautaset, T., Sekurova, O.N., Sletta, H., Ellingsen, T.E., Strøm, A.R., Valla, S., and Zotchev, S.B. (2000). Biosynthesis of the polyene antifungal antibiotic nystatin in *Streptomyces noursei* ATCC 11455: analysis of the gene cluster and deduction of the biosynthetic pathway. Chem. Biol. *7*, 395–403.

Brautaset, T., Borgos, S.E., Sletta, H., Ellingsen, T.E., and Zotchev, S.B. (2003). Site-specific mutagenesis and domain substitutions in the loading module of the nystatin polyketide synthase, and their effects on nystatin biosynthesis in *Streptomyces noursei*. J. Biol. Chem. *278*, 14913–14919.

Bruheim, P., Borgos, S.E., Tsan, P., Sletta, H., Ellingsen, T.E., Lancelin, J.M., and Zotchev, S.B. (2004). Chemical diversity of polyene macrolides produced by *Streptomyces noursei* ATCC 11455 and recombinant strain ERD44 with genetically altered polyketide synthase NysC. Antimicrob. Agents Chemother. *48*, 4120–4129.

Carmody, M., Murphy, B., Byrne, B., Power, P., Rai, D., Rawlings, B., and Caffrey, P. (2005). Biosynthesis of amphotericin derivatives lacking exocyclic carboxyl groups. J. Biol. Chem. *280*, 34420–34426.

Falk, R., Domb, A.J., and Polacheck, I. (1999). A novel injectable water-soluble amphotericin B-arabinogalactan conjugate. Antimicrob. Agents Chemother. *43*, 1975–1981.

Fjærvik, E., and Zotchev, S.B. (2005). Biosynthesis of the polyene macrolide antibiotic nystatin in *Streptomyces noursei*. Appl. Microbiol. Biotechnol. *67*, 436–443.

Gagos, M., Gabrielska, J., Dalla Serra, M., and Gruszecki, W.I. (2005). Binding of antibiotic amphotericin B to lipid membranes: monomolecular layer technique and linear dichroism-FTIR studies. Mol. Membr. Biol. *22*, 433–442.

Hamilton-Miller, J.M. (1973). Chemistry and biology of the polyene macrolide antibiotics. Bacteriol. Rev. *37*, 166–196.

Litchfield, J.T., and Wilcoxon, F.A. (1949). A simplified method of evaluating dose-effect experiments. J. Pharmacol. Exp. Ther. *96*, 99–113.

Maschmeyer, G., Haas, A., and Cornely, O.A. (2007). Invasive aspergillosis: epidemiology, diagnosis and management in immunocompromised patients. Drugs *67*, 1567–1601.

Mazerski, J., Bolard, J., and Borowski, E. (1995). Effect of the modifications of ionizable groups of amphotericin B on its ability to form complexes with sterols in hydroalcoholic media. Biochim. Biophys. Acta *1236*, 170–176.

Nedal, A., Sletta, H., Brautaset, T., Borgos, S.E., Sekurova, O.N., Ellingsen, T.E., and Zotchev, S.B. (2007). Analysis of the mycosamine biosynthesis and attachment genes in the nystatin biosynthetic gene cluster of *Streptomyces noursei* ATCC 11455. Appl. Environ. Microbiol. *73*, 7400–7407.

Ōmura, S., and Tanaka, H. (1984). Production, structure and antifungal activity of polyene macrolides. In Macrolide Antibiotics: Chemistry, Biology, and Practice, S. Omura, ed. (New York: Academic Press), pp. 351–404.

Palacios, D.S., Anderson, T.M., and Burke, M.D. (2007). A post-PKS oxidation of the amphotericin B skeleton predicted to be critical for channel formation is not required for potent antifungal activity. J. Am. Chem. Soc. *129*, 13804–13805.

Paquet, V., and Carreira, E.M. (2006). Significant improvement of antifungal activity of polyene macrolides by bisalkylation of the mycosamine. Org. Lett. *8*, 1807–1809.

Perlin, D.S. (2007). Resistance to echinocandin-class antifungal drugs. Drug Resist. Updat. *10*, 121–130.

Power, P., Dunne, T., Murphy, B., Lochlainn, L.N., Rai, D., Borissow, C., Rawlings, B., and Caffrey, P. (2008). Engineered synthesis of 7-oxo- and 15-deoxy-15-oxo-amphotericins: insights into structure-activity relationships in polyene antibiotics. Chem. Biol. *15*, 78–86.

Sambrook, J., Fritsch, E.F., and Maniatis, T. (1989). Molecular Cloning: A Laboratory Manual (Plainview, NY: Cold Spring Harbor Lab Press).

Seco, E.M., Cuesta, T., Fotso, S., Laatsch, H., and Malpartida, F. (2005). Two polyene amides produced by genetically modified *Streptomyces diastaticus* var. 108. Chem. Biol. *12*, 535–543.

Sekurova, O., Sletta, H., Ellingsen, T.E., Valla, S., and Zotchev, S. (1999). Molecular cloning and analysis of a pleiotropic regulatory gene locus from the nystatin producer *Streptomyces noursei* ATCC11455. FEMS Microbiol. Lett. *177*, 297–304.

Scott, L.J., and Simpson, D. (2007). Voriconazole: a review of its use in the management of invasive fungal infections. Drugs *67*, 269–298.

Silveira, F.P., and Husain, S. (2007). Fungal infections in solid organ transplantation. Med. Mycol. *45*, 305–320.

Sims, C.R., Ostrosky-Zeichner, L., and Rex, J.H. (2005). Invasive candidiasis in immunocompromised hospitalized patients. Arch. Med. Res. *36*, 660–671.

Spanakis, E.K., Aperis, G., and Mylonakis, E. (2006). New agents for the treatment of fungal infections: clinical efficacy and gaps in coverage. Clin. Infect. Dis. *43*, 1060–1068.

Teerlink, T., de Kruijff, B., and Demel, R.A. (1980). The action of pimaricin, etruscomycin and amphotericin B on liposomes with varying sterol content. Biochim. Biophys. Acta *599*, 484–492.

Treshchalin, I.D., Sletta, H., Borgos, S.E., Pereverzeva, E.P., Voeikova, T.A., Ellingsen, T.E., and Zotchev, S.B. (2005). Comparative analysis of in vitro antifungal activity and in vivo acute toxicity of the nystatin analogue S44HP produced via genetic engineering. Antibiot. Khimioter. *50*, 18–22.

Vatsis, K.P., Peng, H.M., and Coon, M.J. (2002). Replacement of active-site cysteine-436 by serine converts cytochrome P450 2B4 into an NADPH oxidase with negligible monooxygenase activity. J. Inorg. Biochem. *91*, 542–553.

Volokhan, O., Sletta, H., Ellingsen, T.E., and Zotchev, S.B. (2006). Characterization of the P450 monooxygenase NysL, responsible for C-10 hydroxylation during biosynthesis of the polyene macrolide antibiotic nystatin in *Streptomyces noursei*. Appl. Environ. Microbiol. *72*, 2514–2519.

Volpon, L., and Lancelin, J.M. (2002). Solution NMR structure of five representative glycosylated polyene macrolide antibiotics with a sterol-dependent antifungal activity. Eur. J. Biochem. *269*, 4533–4541.

Zotchev, S.B. (2003). Polyene macrolide antibiotics and their applications in human therapy. Curr. Med. Chem. *10*, 211–223.

Zotchev, S., Haugan, K., Sekurova, O., Sletta, H., Ellingsen, T.E., and Valla, S. (2000). Identification of a gene cluster for antibacterial polyketide-derived antibiotic biosynthesis in the nystatin producer *Streptomyces noursei* ATCC 11455. Microbiology *146*, 611–619.

